IEEE Access
Multidisciplinary | Rapid Review | Open Access Journal

Received 12 March 2023, accepted 22 March 2023, date of publication 29 March 2023, date of current version 10 April 2023.

Digital Object Identifier 10.1109/ACCESS.2023.3262776

RESEARCH ARTICLE

Design Process of Post-Assembly 3-Times Magnetizer for 10-Poles of Flux Concentrated Rotor Considering Eddy Current Effect

SEONG-JIN KWON[1], BYEONG-HWA LEE[2], (Member, IEEE), KYU-SEOB KIM[3], AND JAE-WOO JUNG[4], (Member, IEEE)

[1]Department of Automotive Engineering, Yeungnam University, Gyeongsan 38541, South Korea
[2]Korea Automotive Technology Institute, Daegu 43011, South Korea
[3]Department of Automotive Engineering, Gyeongsang National University, Jinju 52725, South Korea
[4]Department of Electrical Engineering, Daegu University, Gyeongsan 384543, South Korea

Corresponding author: Jae-Woo Jung (jjw@daegu.ac.kr)

This work was supported by the National Research Foundation of Korea (NRF) grant funded by the Korea Government (MSIT) under Grant NRF2021R1G1A095642.

ABSTRACT The post-assembly magnetizer for flux concentrated rotor of permanent magnet synchronous motor is dealt with in this paper. The design process of a magnetizer that is able to fully magnetize the permanent magnet (PM) inserted rotor core assembly within 3-times is discussed. The number of turns of the Main-pole winding and the Inter-pole winding was determined to maximize the magnetization ratio in each magnetization stage. At the same time, demagnetization characteristic is also examined. When the magnetizer is designed, the number of turns of winding is determined considering the eddy current generated in the core. The magnetization ratio of the PM considering the eddy current effect is compared with the magnetization ratio of the designed magnetizer when the eddy current effect is ignored. Finally, the properties of the finally designed magnetizer are verified through fabricated magnetizer and experiments.

INDEX TERMS Demagnetization, eddy currents, ferrite magnet flux concentrated rotor, magnetization.

I. INTRODUCTION

As industrialization progresses, the use of rare earth metals in various fields is increasing. In particular, research has been conducted on interior permanent magnet synchronous motors (IPMSM) using Nd-Fe-B permanent magnet (PM) to increase the power density and efficiency of motors [1], [2], [3], [4]. However in 2010, the surge in neodymium and dysprosium prices became a catalyst for motor designers to study rare earth free motors. Various types of motors that do not use rare earth metals such as aluminum die-casting induction motors and synchronous reluctance motors have been studied, but owing to their low power factor, there are limits to achieving the same performance as IPMSM using the rare earth metals [5], [6]. On the other hand, studies for reducing heavy rare earth metals in PM have been actively conducted in terms of material engineering [7], [8], [9]. Among the various efforts for realization of rare earth free motors, flux concentrated permanent magnet synchronous motors (FC-PMSM) using ferrite PM can achieve high efficiency as well as high power factor. Moreover, it can be designed to have almost same torque density as conventional IPMSM [10], [11], [12]. In relation to this, research has been reported on motors employing nonmagnetic materials such as high manganese steel or stainless steel [13], [14]. In Hae-Jung Kim's study, various PM shapes were applied to maximize magnetic flux and to increase the torque density by using magnetic flux flowing through axial direction [15]. Ji-Min Kim's research has improved the torque density by using a segment type core that has completely removed the bridge of the rotor [16]. Wataru proposed a 50 kW automotive drive motor as a ferrite magnet FC-PMSM [17]. In the study of Sung-Il Kim, a FC-PMSM was implemented by applying two PMs with different pole shapes to one pole [18]. Mohammad, on the other hand, proposed a wing shaped spoke type rotor [19]. Hyungkwan Jang introduced a method to improve torque

The associate editor coordinating the review of this manuscript and approving it for publication was Amin Mahmoudi.

characteristics by reducing leakage flux through bridge shape design [20]. Jae-Woong Jung presented a study on improving the torque characteristics of FC-PMSM by applying a PM overhang [21]. Various types of rotors using ferrite PM have been developed, but all of them are manufactured by inserting magnetized PM into the rotor core except [21]. In [21], the magnetization after assembly of the 8-pole rotor was mentioned. However, it is different from the number of poles dealt with in this paper and does not deal with magnetization analysis. In the case of using the pre-magnetized PM, mass production is possible, but cleanliness management is difficult to prevent magnetic dust from sticking to the magnetized PM. Also, in the process of inserting PM into the rotor core, the probability of cracking in the PM is high.

Research on magnetization after rotor assembly has been conducted on surface-mounted permanent magnet synchronous motors (SPMSM) rather than flux concentrated rotors. In 1992, G. W. Jewll of Sheffield University published an external rotor type brushless DC motor with Nd-Fe-B PM for 4-pole magnetization through a magnetization using stator assembly [22]. Several studies have been conducted on the post-assembly magnetization of SPMSM since the study [22]. In particular, Min-Fu and David G. Dorrel published several studies on how to magnetize the PM in rotor with several times using the electromagnetic force of the stator after assembling the rotor into the stator assembly [23], [24], [25], [26]. However, since it is not a study on magnetic flux concentrated type rotor, it is difficult to use it as references for design of a rare earth free PMSM with flux concentrated type of rotor. Min-Jae Jeong proposed an I spoke-type PMSM that can improve the salient pole ratio. In addition to reviewing the motor performance, a method to improve the magnetization characteristics was proposed. However, the content related to magnetization is a small part of the paper and the effect of eddy current in the magnetic circuit was not considered [27], [28].

On the other hand, magnetizers for FC-PMSM have been studied. Gyu-Seop Kim has established the magnetization analysis process of rotor of PMSM using ferrite PM [29]. The method of calculating the inductance by considering the magnetic saturation of yoke and then calculating the magnetizing current by the analytic method was discussed. However, they did not consider the eddy currents generated in the core during magnetization. In some studies, only the eddy currents inside the PM were considered for magnetization analysis [30], [31]. In article published by Hyun-Soo Seol [32], the 3-times magnetizer has been proposed and discussed of its structure and basic principle. In the previous result [32], only the operating principle and concept of the 3-times magnetizing method can be found, but the process of designing the magnetizer cannot be confirmed. Most of all, previous article does not mention the method of determining the number of winding turns. In addition, the eddy current effect was not considered in the analysis of the magnetization ratio.

In order to reinforce what was lacking in previous research work, we discuss the design process of the 3-times magnetizer for the flux concentrated rotor with 10-poles. Unlike other studies that ignore the effects by the eddy currents, this study considers the eddy current effect on magnetization. Before beginning to discuss the design process, the magnetization ratio according to various method that is taking into account eddy current effect has been examined. After we examine the magnetization ratio by applying various methods of eddy current calculation and find eddy current calculation method that best reflects actual phenomenon by comparing with experimental results. The description of the process of designing a magnetizer considering eddy currents deals with the process of determining the number of windings turns of the Main-pole and the Inter-pole to maximize the magnetization ratio. At the same time, the number of winding turns of both poles is determined, in which PM magnetized in the previous step is not demagnetized. In conclusion, although the maximum voltage is required, the determination of the appropriate charging voltage required for magnetization is also explained. Finally, we present the results of the magnetization analysis using the designed magnetizer, and then verify the reliability of the magnetizer designed through the proposed process in comparison with the magnetization ratio obtained through the experiment.

II. EXAMINE OF PROTOTYPE

Before explaining the magnetization design process, this chapter describes the basic specifications and rotor shape of the target motor. Magnetization was performed using a prototype designed based on the existing research results [32]. Based on the results of the magnetization of the prototype, analysis of the magnetizer is established.

A. STRUCTURE OF FLUX CONCENTRATED ROTOR AND PROTOTYPE OF MAGNETIZER

The rotor has an outer diameter of 56.0 mm and an axial length of 21.5 mm and is applied to a 500 watt motor. In order to increase the torque density, the rotor cores are stacked with two types of core in an intersection and are described details in [33]. In the existing literature, the I spoke type PMSM has a high saliency ratio, but it requires twice as many PMs per pole, which is disadvantageous in terms of process management and cost reduction [27], [28]. Therefore, the design was carried out with a general spoke-shaped FC -PMSM. In addition to the dimension information of the poles and rotors mentioned above, the sizes and grades of the PMs are shown in Fig. 1 and Table 1. The ferrite PM inserted in the rotor core is an NMF-9G manufactured by Hitachi Metals.

The magnetic properties of the material are shown in Fig. 2. The initial magnetization curve for one quadrant and magnetization ratio according to the magnetizing field are shown in Fig. 2 (a) and (b), respectively. The magnetic field is mapped in the PM after the magnetic circuit analysis using the finite element analysis (FEA), and the magnetization

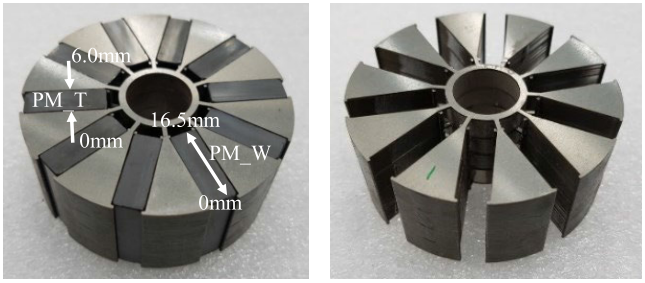

FIGURE 1. Flux concentrated rotor. (a) With ferrite PM (b) Rotor core only.

TABLE 1. Information of FC-PMSM rotor and magnetizer.

Title	Value	Description
No. of poles	10	-
Rotor O.D. [mm]	56.0	-
Stack length [mm]	21.5	-
Rotor core grade	S60	Laminated core
PM_L	13.5	Length of PM
PM_T	6.5	Thickness of PM
PM grade	NMF-9G	Hitachi metals
Remanence flux density (*Br*) [T]	0.41	20℃
Magnetizer core grade	S18	-
Capacitance [μF]	2000	-
Max. charging voltage [V]	2000	DC voltage

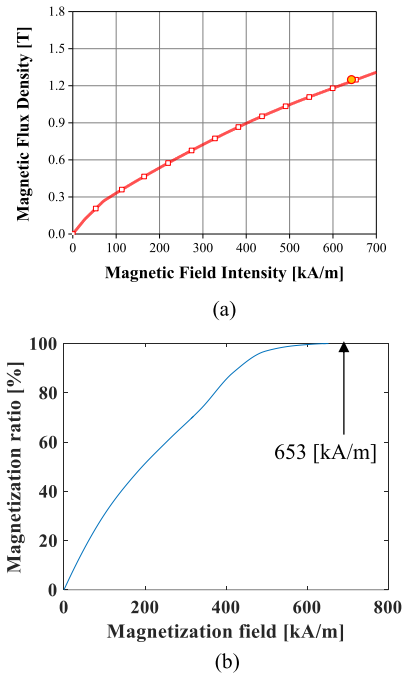

FIGURE 2. Characteristics of ferrite PM (Hitachi metals NMF-9G). (a) Initial B-H curve (b) Magnetization ratio according to magnetization.

ratio is calculated by comparing with the magnetic field in Fig. 2 (b).

The prototype of magnetizer is based on the know-how accumulated by the magnetizer manufacturer with reference to the existing research [32], and is shown in Fig. 3. It consists

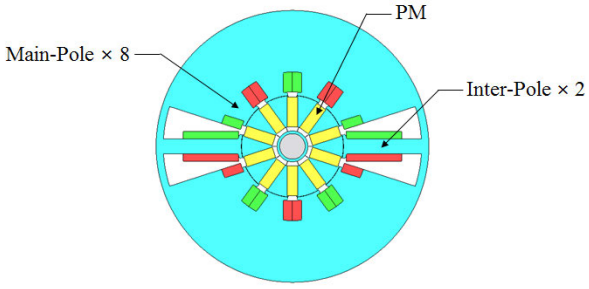

FIGURE 3. Configuration of initial model of 3-times magnetizer.

of 8 Main-poles and 2 Inter- poles. The Main-pole and the Inter-pole have 4-turns and 8-turns, respectively. The 8 Main poles of the magnetizer are for magnetizing the permanent magnet. On the other hand, the 2 Inter poles properly secure the leakage path during magnetization to prevent the demagnetization of the previously magnetized permanent magnet [32]. Because of the condition of the magnetizer, which has no significant restriction on the space, slot space is enough to wind the coil. The specification of the power supply is also described in Table 1. The circuitry of the power unit that makes up the magnetizer is the same as described in [32].

B. MAGNETIZATION RATIO OF ROTOR MAGNETIZED BY PROTOTYPE

The magnetization ratio of PM was calculated by using two-dimensional (2-D) FEA without consideration of eddy current effect as previous research results. Figure 4 (a) shows the magnetization field calculated inside the PM when the magnetizing current is applied. Figure 4 (b) shows the remanence flux density of the PM. Using the calculated magnetization ratio by comparing the magnetization field calculated through FEA and Fig. 2 (b), it was converted into remanence flux density value. As shown in Fig. 4 (b), analysis value of the magnetization ratio by prototype is 100 % satisfied.

An experiment was performed to verify the magnetization ratio of the rotor magnetized by the prototype magnetizer. A reference model is needed to confirm the magnetization ratio of the PM that is magnetized through 3-times post assembly magnetization. Therefore, we made a sample that pre- magnetized PM is inserted into the rotor core to assemble the rotor, and this will be referred to as a primary sample. A prototype magnetizer was fabricated as shown in Fig. 5 (a). Total surface magnetic flux of the rotor was measured after 3-time magnetization. Fig. 5 (b) shows the total surface magnetic flux of the primary sample and (c) shows the total surface magnetic flux of the sample that magnetized through 3-times magnetization. It can be seen that the 3-times magnetization result is 69.4 % compared to the primary sample.

Based on the experimental results, the analysis of magnetization ratio using previous analysis method could not exactly predict the magnetization ratio of the FC-PMSM rotor in which magnetized by 3-times magnetizer. Therefore, it is necessary to establish an analysis method that can accurately predict magnetization ratio.

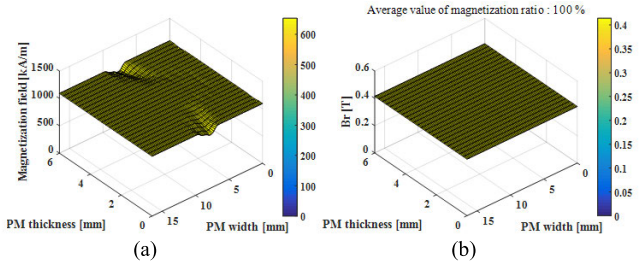

FIGURE 4. Calculated magnetization field and remanance flux density of rotor magnetized by prototype. (a) Magnetization field (b) Remanence flux density.

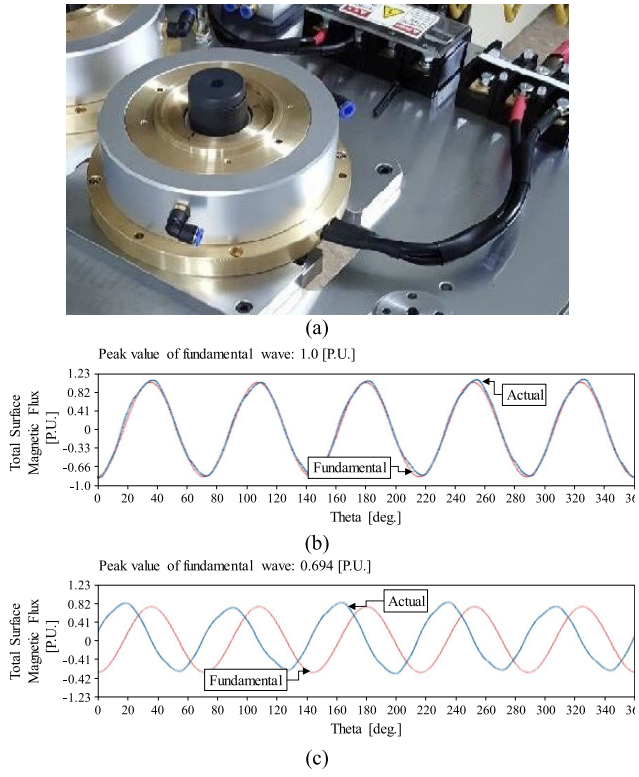

FIGURE 5. Experimental results of magnetization with prototype (Total surface magnetic flux). (a) Experiment set-up (b) Rotor surface magnetic flux of primary sample (c) Rotor surface magnetic flux of post assembly magnetized sample.

C. MAGNETIZATION RATIO OF ROTOR MAGNETIZED BY PROTOTYPE

Most of the studies published previously related to magnetizer for SPMSM ignore the eddy current effect when analyzing the magnetization ratio of PM. This is because the eddy current generated in the magnetic core does not significantly affect the magnetization ratio because the PM is in contact with the air-gap. However, the influence of the eddy current generated in the magnetizer and the rotor core cannot be ignored in case of FC-PMSM because the eddy current generated in the magnetic core directly interferes with the flow of magnetic flux required for magnetization.

When the eddy current is not considered in the magnetization analysis, the desired magnetization ratio is not be obtained in actual experiment as described above. In order to estimate the eddy currents of the magnetizer and the rotor core made of laminated cores, a three-dimensional FEA is required in which all the laminated shapes are reflected. However, because of the enormous increase in mesh size, the interpretation is almost impossible. In order to overcome this problem, this paper deals with the approach through 2-D FEA.

In order to compare the effect of eddy current on the magnetization ratio, the magnetization ratio for two methods was analyzed.

1) Method-1: First, the magnetic circuit of the magnetizer is analyzed through transient analysis of 2-D FEA. At this time, the core is assumed to be solid and the conductivity is set to zero. Next, a 1-D eddy current analysis is carried out. In this analysis, the axial thickness of the steel sheet is considered [34]. The influence of Eddy current is reflected in the magnetic circuit and the magnetization rate is calculated.

2) Method-2: Assign conductivity in the core. Calculate the magnetization ratio using the transient analysis of 2-D FEA with the core is set as a solid. It is assumed that the insulation between the laminated core sheets cannot be maintained.

In the Method-1, the magnetization ratio is calculated under the condition that electrical insulation between the laminated steel sheets is perfect. In the Method-2, the eddy current is calculated in a state where the lamination conditions are neglected. The magnetization ratio of PM was calculated by using two analysis methods as shown in Fig. 6. The magnetization ratio of Method-1 is 100 % satisfied because there is no significant eddy current effect. However, it is confirmed that the magnetization ratio of Method-2 in which the eddy current is largely calculated is only about 69.8 %.

From the experimental experience, it is judged that it is difficult to expect the effect of reducing the eddy current through the use of the laminated steel sheet as there is no significant difference in magnetization ratio depending on the use of the laminated steel sheet in the magnetizer. Based on comparison of experimental result and analysis result, Method-2 is the most appropriate analysis method for design of the 3-times magnetizer.

Figure 7 shows the eddy current vectors calculated by Method-1 and Method-2. Based on the eddy current vector of Fig. 7, it can be concluded that the eddy current calculated by method -2 has the greatest effect on the magnetization ratio. Because the eddy current vector calculated through method-1 is distributed in the horizontal direction on the steel plate, while the eddy current vector calculated through method-2 is perpendicular to the steel plate.

III. DESIGN OF MAGNETIZER CONSIDERING EDDY CURRENT EFFECT

In order to magnetize the PM, the energy stored in the capacitor is discharged to the coil in a short period of time after

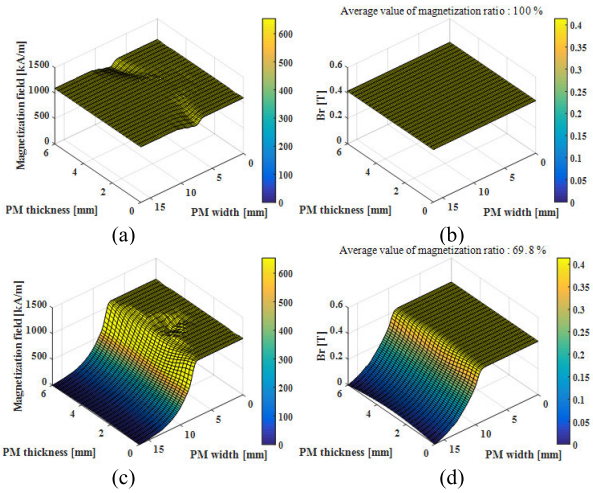

FIGURE 6. Calculated magnetization field and remanance flux density according to calculation method of eddy current. (a) Magnetization field by Method-1 (b) Remanence flux density by Method-1 (c) Magnetization field by Method-2 (d) Remanence flux density by Method-2.

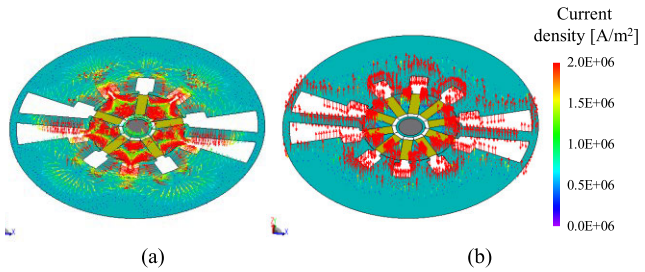

FIGURE 7. Eddy current distribution according to analysis method. (a) Method-1 (b) Method-2.

charging the DC voltage to the capacitor. Impulse shaped current is applied within a few milliseconds, so that an eddy current is generated in the magnetic core. In this chapter, magnetizer is designed considering the eddy current effect and the result is discussed. Then, the comparison of the magnetization analysis results of the designed magnetizer is discussed according to the eddy current analysis method.

A. DESIGN PROCESS OF 3-TIMES MAGNETIZER

The process of designing the magnetizer is relatively complicated because it is a process of performing the magnetization three times. The magnetizer design process is shown in Fig. 8. The design process consists of a total of 4-steps. The design process of the magnetizer is reversed to the order in which the actual magnetization is performed. The PM is assigned an ID, and the target PM of each step is different. The total magnetizer design process is done through the 2-D FEA.

1) Step-1: Perform the core shape design of magnetizer based on general 1-time magnetizer. The shape of Main-pole and Inter-pole is designed with reference to [32].

2) Step-2: Step-2 is a design step for performing the third magnetization. Remanence flux density (Br) values are given to eight poles (No. 1, No. 2, No. 3, No. 4, No. 6, No. 7, No. 8, No. 9) and two poles (No. 5, No. 10) are assigned as the target of the magnetization. In this step, the magnetization ratio as well as the demagnetization ratio should be examined, unlike other steps. First, the number of turns of the Main-pole and the Inter-pole is determined considering the slot space. At this time, the number of winding turns of the Main-pole and the Inter-pole is set to be the same. Next, the magnetization of the target PM is checked while increasing the voltage. If the target poles are 100 % magnetized, check to see if demagnetization has occurred at the pole with the Br value assigned. If demagnetization occurs, increase the number of turns of Inter-pole only and examine the rate of both magnetization and demagnetization. If the applied voltage reaches the voltage limit, increase the number of turns of main-pole. Repeating this process can determine the number of turns of the Main-pole and the Inter-pole, in which the magnetizing target pole is completely magnetized and the pole to which the Br value is assigned is not demagnetized.

3) Step-3: This is the second magnetization state, and there are four magnetizing target poles (No. 2, No. 4, No. 7, No. 9). The number of poles to which the Br value is assigned is also four (No. 1, No. 3, No. 6, No. 8). The rotor shall be rotated after the mechanical angle of 72 degrees to the rotor position in step 2. While lowering the voltage value based on the voltage value determined in Step-2, find the minimum charging voltage at which the pole's magnetization ratio reaches 100 %. Unlike Step-2, there is no need to review of demagnetization. This is because the Main-pole and Inter-pole winding ratios to prevent demagnetization of the Br assigned poles were already determined in step 2.

4) Step 4: Step-4 is the first state of 3-times magnetization. First, rotate the rotor at 144 degrees in Step 3. Only 4 poles are magnetized targets (No. 1, No. 3, No. 6, No. 8), and no pole has Br value assigned. Based on the charging voltage determined in Step-3, while lowering the value; find the lowest charging voltage at which the magnetization ratio of the target pole is 100 %.

The main purpose of this design process is to determine the number of the Main-pole and the Inter-pole to prevent demagnetization in the pre-magnetized poles, while at the same time completely magnetizing the target poles. It also finds the minimum charge voltage required at each step. In this design process, eddy current effect must be considered by applying Method-2 described in the previous chapter.

TABLE 2. Comparison of design result according to eddy current calculation method.

Title	Model-1 (@ Without eddy current)	Model-2 (@ Method-2)
No. of turns for main pole	4	17
No. of turns for inter pole	8	34
Conductor O. D. [mm]	2.0	1.1
Charging voltage in First-shot [V]	500	2000
Charging voltage in Second-shot [V]	1400	2000
Charging voltage in Third-shot [V]	1600	2000

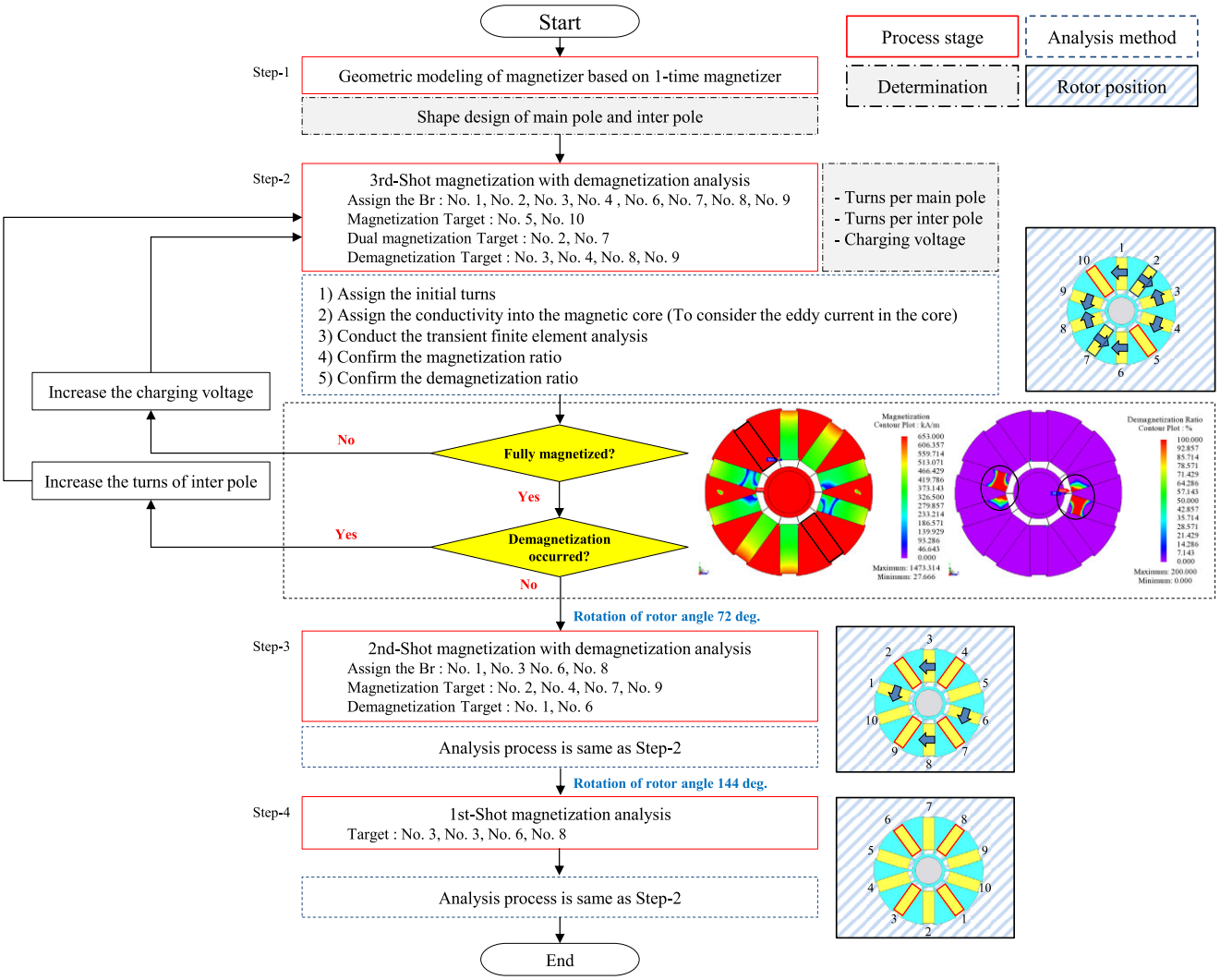

FIGURE 8. Design process of 3-Times magnetizer for FC-PMSM.

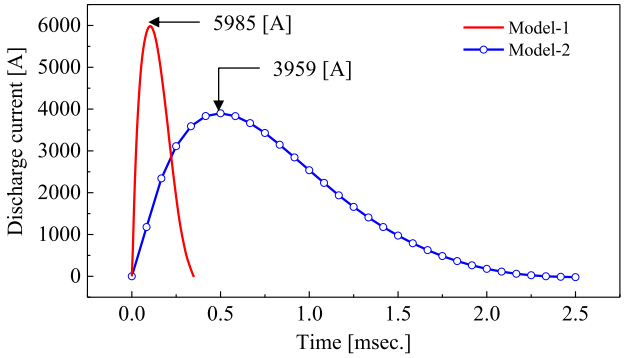

FIGURE 9. Comparison of discharging current between Model 1 and Model 2.

Table 2 compares the number of turns of the magnetizer with the required voltage according to the eddy current analysis method. Model-1 is a magnetizer designed without considering eddy currents. In Model-2 in which the eddy current is considered by using Method 3, the number of turns is increased more than 4-times compared to Model 1. As shown in described in (1) and (2), if the number of turns of the winding in the magnetic circuit increases, the inductance increases in proportion to the square of the number of turns. Therefore, the discharge time is increased during the current discharge, so that the eddy current can be reduced.

$$L = N^2 \Big/ R_M \tag{1}$$

$$i(t) = \frac{V_0 \cdot t}{L} e^{\frac{-R}{2L} \cdot t} \tag{2}$$

here, L is circuit inductance, N is number of turn, R_M is magnetic resistance, $i(t)$ is discharge current, V_0 is initial voltage on the capacitor, and R is circuit resistance.

Fig. 9 shows the discharge current waveform of the designed model. It can be seen that the discharge time of the designed model was increased up to 7-times under the condition that the eddy current was considered. Although the

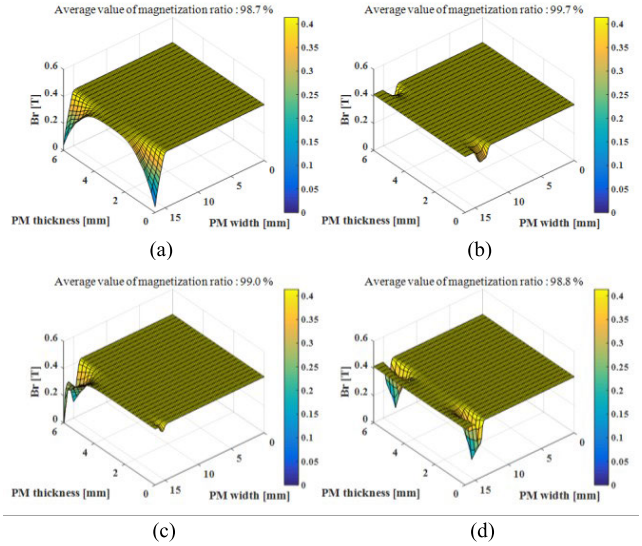

FIGURE 10. Calculated remanance flux density of Model-2. (a) No. 1, No. 3, No. 6, No. 8 (b) No. 2, No. 9 (c) No. 4, No. 7 (d) No. 5, No. 10.

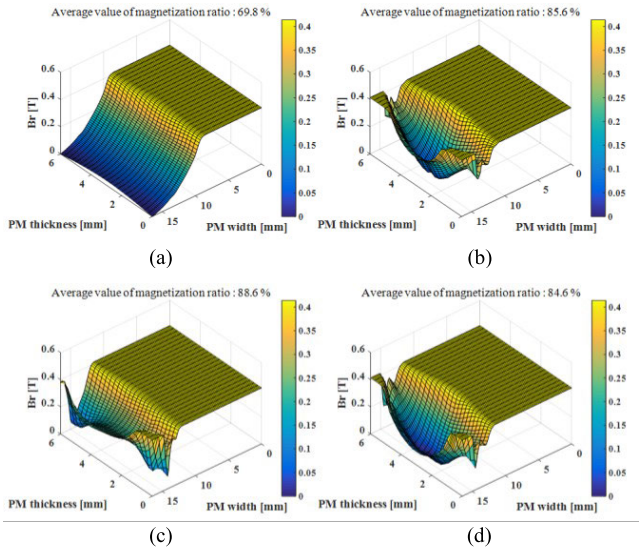

FIGURE 11. Calculated remanance flux density of Model-1. (a) No. 1, No. 3, No. 6, No. 8 (b) No. 2, No. 9 (c) No. 4, No. 7 (d) No. 5, No. 10.

applied voltage is increased, the maximum current value of Model-2 is lower because of the increase of the number of turns. For comparison under the same conditions, the results of FEA were compared by applying the eddy current analysis Method-2 to both models.

B. EXAMINE OF MAGNETIZATION RATIO ON EACH STEP

In order to confirm the magnetization characteristics of Model-2 derived from the magnetizer design process, 3-times magnetization analysis was performed and compared with the magnetization characteristics of Model-1. Magnetization characteristics as well as demagnetization characteristics of pre-magnetized PM were also confirmed. In First-shot and Third-shot magnetization, the magnetization pattern of the PM is symmetrical, but not in the case of the Second-shot. Therefore, a totally four of Br maps were calculated and compared.

In each Fig. 10 and 11, (a) is the result of Br map of PM No. 1, No. 3, No. 6 and No. 8 obtained by First-shot magnetization. In (b) shows the Br map of the PM No. 2 and 9. And (c) shows the Br map of the PM No. 4 and 7. Both of (b) and (c) is obtained by the Second-shot magnetization. Finally, Fig. 10 and 11 (c) shows the results of Br map of PM ID No. 5 and No. 10 obtained through Third-shot. The average value of the magnetization ratio of Model-1 is 79.68 % and the average value of Model-2 is 98.98 %, which shows that the model-2 is satisfying the magnetization ratio. All analyzed magnetization ratio for PM is put into the Table 3. Fig. 12 is a graph comparing the eddy current loss of the core.

The maximum value of eddy current loss of Model-1 is smaller than that of Model-2. However, if the voltage of

TABLE 3. Magnetization ratio on each PM.

PM ID	Model-1 [%]	Model-2 [%]
No. 1, No. 3, No. 6, No. 8	69.8	98.7
No. 2, No. 9	85.6	99.7
No. 4, No. 7	86.6	99.0
No. 5, No. 10	84.6	98.8
Total average	79.68	98.98

Model-1 is 2000 V, which is equal to the required voltage of Model-2, eddy current loss of Model-1 is increased 10-times compared with Model-2. Considering the fact that model-1 is larger than model-2 by 1.7 times in Ampere-Turns when applying the same 2000 V to both models, the eddy current loss of model-1 is much greater than that of model-2. For reference, according to FEA results, when 2000 V is applied to Model-1, the discharge current is 115 kA during First-shot. The fact that the charging voltage required for Model-2 is 4 times higher than that of Model-1 can act as a disadvantage in terms of insulation of magnetizer windings. This is because the higher the discharge voltage, the stronger the withstand voltage requirement between the winding and the magnetizing yoke. Therefore, difficulties in manufacturing the magnetizer are added. However, in this study, the manufacturing point of view was excluded and the focus was on the magnetization performance of the magnetizer.

On the other hand, the effect of an Inter-pole to prevent the demagnetization effect is described in [32]. Since we found the winding ratio to prevent the demagnetization through the magnetizer design process, we can confirm that the demagnetization ratio satisfies 0 %.

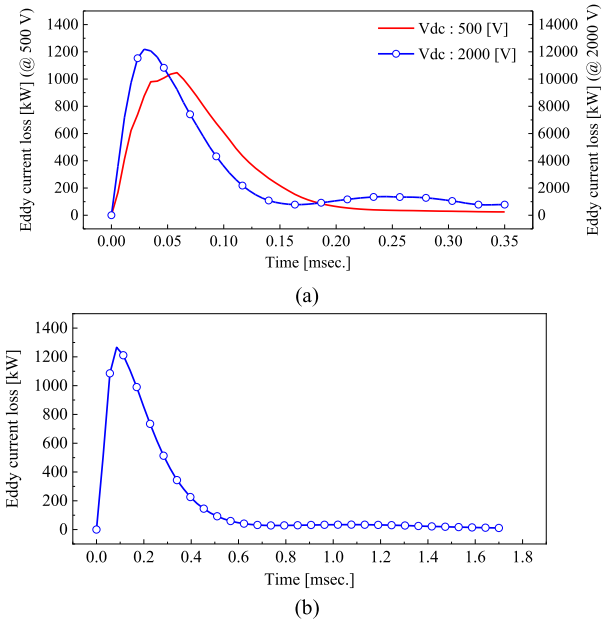

FIGURE 12. Eddy current loss in magnetizer. (a) Model-1 (b) Model-2.

IV. FABRICATION AND EXPERIMENT

A prototype was fabricated as shown in Fig. 13 (a) to verify the magnetization of model 2 designed through the proposed magnetization design process. The final shape of the assembled magnetizer is similar to Fig. 6 (a). A reference value is needed to verify the magnetization ratio. Therefore, the surface magnetic flux of the rotor assembly in which the pre-magnetized PM was inserted into the rotor core was measured as shown in Fig. 13 (b). The test results in Fig. 13 (b) are the same as those in Fig. 5 (b) and re-experiments were performed to ensure the same test environment. After the frequency analysis of the magnetic flux on the measured rotor surface, it was confirmed that the fundamental wave component is 1.0 P.U.. Fig. 13 (c) shows the result of measuring the surface magnetic flux density of the rotor with post assembly 3-times magnetization. As a result of the measurement, frequency analysis was performed and it was confirmed that the fundamental wave component satisfies 0.987 P.U.. It was confirmed that the magnetization ratio through the post assembly 3-times magnetizer was 98.7 %, based on the two magnetic flux quantities. For the reference, the performance of the motor is determined by the fundamental component of the air-gap magnetic flux density. Therefore, the magnetization ratio is calculated based on the flux value of the fundamental component.

On the other hand, the actual waveform is obtained by applying a moving average filter to the raw data obtained by measuring the magnetic flux on the surface of the rotor. Frequency analysis was performed on the actual waveform to identify the fundamental component. The fact that there are some asymmetric areas in the actual waveform is due to the average section setting when applying the moving average filter.

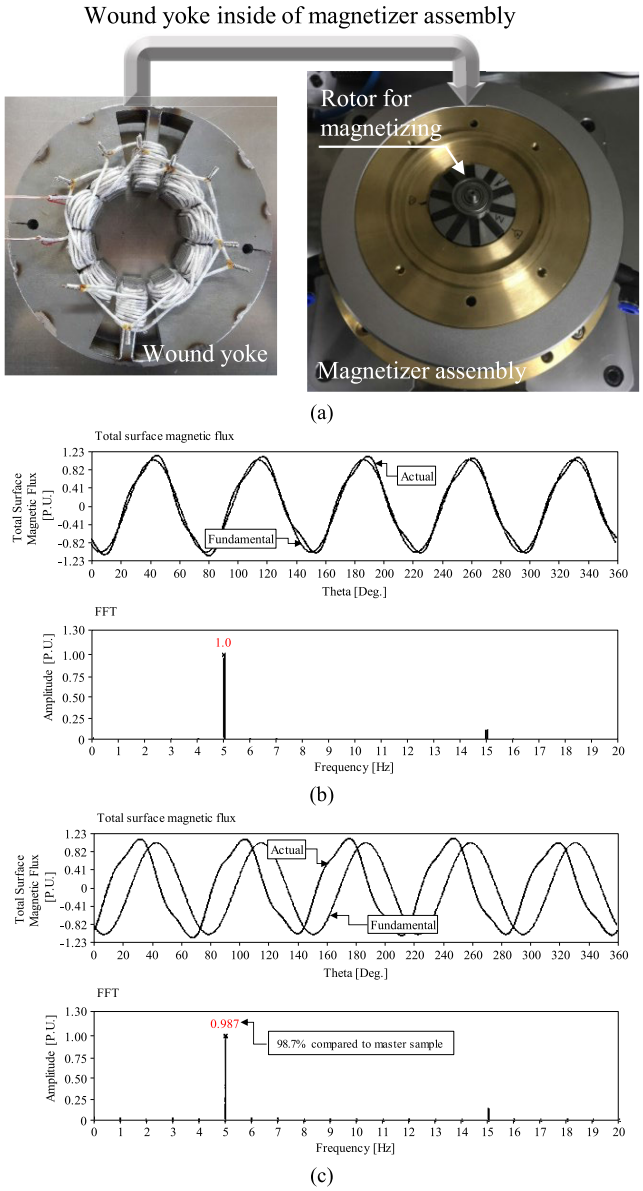

FIGURE 13. Experimental results of magnetization. (a) Fabricated wound yoke and magnetizer assembly (b) Magnetization result of Primary sample (c) Magnetization result of Designed sample.

V. CONCLUSION

Among rare-earth free motors, FC-PMSM using ferrite PM is one of the best candidates for a small-sized motor of several hundred watts. However, because of the structural characteristics of the flux concentrated rotor, it is difficult to complete the magnetization after assembly. In order to overcome this problem, 3-times magnetizers have been studied. In this paper, the design process for determining the number of winding turns of Main-pole and Inter-pole, which is most important when designing a 3-times magnetizer, is discussed. In general SPMSM, there is no difficulty in predicting magnetization performance without considering the effect of eddy current in magnetization. This is because the magnetic field

reaches the PM immediately after passing through the air-gap. However, flux concentrated rotor is different. Therefore, the method of considering the eddy current in the design of the 3-Times magnetizer after assembly was examined through experiments and FEA. Then it is reflected into the design process. The performance of the designed magnetizer was confirmed by calculating the *Br* map of PM using FEA. Finally, the validity of the design process of the magnetizer was verified through experiments.

In this paper, the design of the magnetizer considering the eddy current of the core is discussed, but there remain some considerations in the design process. Mechanical parts such as coil stress caused by electromagnetic force and thermal problem occurring in coil when electric current is discharged will also be examined in the future. In the other hand, with regard to the analysis Method-2 described in Section II, a study will be conducted to theoretically and experimentally analyze the induced voltage generated in the magnetic circuit when the impulse voltage is applied and the insulation performance of the electrical steel sheet.

REFERENCES

[1] F. Mwasilu, H. T. Nguyen, H. H. Choi, and J.-W. Jung, "Finite set model predictive control of interior PM synchronous motor drives with an external disturbance rejection technique," *IEEE/ASME Trans. Mechatronics*, vol. 22, no. 2, pp. 762–773, Nov. 2016.

[2] P. Zhang, Y. G. Sizov, M. Li, M. D. Ionel, A. O. N. Demerdash, J. S. Stretz, and W. A. Yeadon, "Multi-objective tradeoffs in the design optimization of a brushless permanent-magnet machine with fractional-slot concentrated windings," *IEEE Trans. Ind. Appl.*, vol. 50, no. 5, pp. 3285–3294, Mar. 2014.

[3] X. Liu, H. Chen, J. Zhao, and A. Belahcen, "Research on the performances and parameters of interior PMSM used for electric vehicles," *IEEE Trans. Ind. Electron.*, vol. 63, no. 6, pp. 3533–3545, Feb. 2016.

[4] K.-C. Kim, D.-H. Koo, J.-P. Hong, and J. Lee, "A study on the characteristics due to pole-arc to pole-pitch ratio and saliency to improve torque performance of IPMSM," *IEEE Trans. Magn.*, vol. 43, no. 6, pp. 2516–2518, Jun. 2007.

[5] Y. Wang, D. Ionel, G. D. Dorrell, and S. Stretz, "Establishing the power factor lamination for synchronous reluctance machines," *IEEE Trans. Magn.*, vol. 51, no. 11, Nov. 2015, Art. no. 8111704.

[6] A. Ukil, R. Bloch, and A. Andenna, "Estimation of induction motor operating power factor from measured current and manufacturer data," *IEEE Trans. Energy Convers.*, vol. 26, no. 2, pp. 699–706, Jun. 2011.

[7] S. Hirosawa, H. Tomizawa, S. Mini, and A. Hamamura, "High-coercivity Nd-Fe-B-type permanent magnets with less dysprosium," *IEEE Trans. Magn.*, vol. 26, no. 5, pp. 1960–1962, Sep. 1990.

[8] S. Sugimoto, M. Nakamura, M. Matsuura, Y. Une, H. Kubo, and M. Sagawa, "Enhancement of coercivity of Nd-Fe-B ultrafine powders comparable with single-domain size by the grain boundary diffusion process," *IEEE Trans. Magn.*, vol. 51, no. 11, Nov. 2015, Art. no. 21010044.

[9] L. Chen, X. Cao, S. Guo, J. Di, G. Ding, C. Yan, R. Chen, and A. Yan, "Coercivity enhancement of dy-free sintered Nd-Fe-B magnets by grain refinement and induction heat treatment," *IEEE Trans. Magn.*, vol. 51, no. 11, Nov. 2015, Art. no. 2101403.

[10] J.-R. Riba, C. López-Torres, L. Romeral, and A. Garcia, "Rare-earth-free propulsion motors for electric vehicles: A technology review," *Renew. Sustain. Energy Rev.*, vol. 57, pp. 367–379, May 2016.

[11] A. El-Refaie, T. Raminosoa, P. Reddy, S. Galioto, D. Pan, K. Grace, J. Alexander, and K. K. Huh, "Comparison of traction motors that reduce or eliminate rare-earth materials," *IET Elect. Syst. Transp.*, vol. 7, no. 3, pp. 207–214, Sep. 2017.

[12] Z. Wang, T. W. Ching, S. Huang, H. Wang, and T. Xu, "Challenges faced by electric vehicle motors and their solutions," *IEEE Access*, vol. 9, pp. 5228–5249, 2021.

[13] H.-W. Kim, K.-T. Kim, Y.-S. Jo, and J. Hur, "Optimization methods of torque density for developing the neodymium free SPOKE-type BLDC motor," *IEEE Trans. Magn.*, vol. 49, no. 5, pp. 2173–2176, May 2013.

[14] Y. Demir, O. Ocak, and M. Aydin, "Design, optimization and manufacturing of a spoke type interior permanent magnet synchronous motor for low voltage-high current servo applications," in *Proc. Int. Electr. Mach. Drives Conf.*, Chicago, IL, USA, May 2013, pp. 9–14.

[15] H.-J. Kim, D.-Y. Kim, and J.-P. Hong, "Structure of concentrated-flux-type interior permanent-magnet synchronous motors using ferrite permanent magnets," *IEEE Trans. Magn.*, vol. 50, no. 11, Nov. 2014, 8206704.

[16] J.-M. Kim, S.-H. Chai, M.-H. Yoon, and J.-P. Hong, "Plastic injection molded rotor of concentrated flux-type ferrite magnet motor for dual-clutch transmission," *IEEE Trans. Magn.*, vol. 51, no. 11, Nov. 2015, Art. no. 8205204.

[17] W. Kakihara, M. Takemoto, and S. Ogasawara, "Rotor structure in 50 kW spoke-type interior permanent magnet synchronous motor with ferrite permanent magnets for automotive applications," in *Proc. IEEE Energy Convers. Congr. Expo.*, Denver, CO, USA, Sep. 2013, pp. 606–613.

[18] S.-I. Kim, S. Park, T. Park, J. Cho, W. Kim, and S. Lim, "Investigation and experimental verification of a novel spoke-type ferrite-magnet motor for electric-vehicle traction drive applications," *IEEE Trans. Ind. Electron.*, vol. 61, no. 10, pp. 5763–5770, Oct. 2014.

[19] M. M. Rahman, K.-T. Kim, and J. Hur, "Design and optimization of neodymium-free SPOKE-type motor with segmented wing-shaped PM," *IEEE Trans. Magn.*, vol. 50, no. 2, pp. 865–868, Feb. 2014.

[20] H. Jang, S. Cho, K. S. Lee, Y. J. Oh, and J. Lee, "Design of power density improvement by applying novel shape of slit and notch to outer rib of rotor of spoke-type permanent magnet synchronous motor," *Open Electr. Electron. Eng. J.*, vol. 12, no. 1, pp. 75–85, Oct. 2018.

[21] J.-W. Jung, D.-H. Jung, and J. Lee, "A study on the design method for improving the efficiency of spoke-type PMSM," *IEEE Trans. Magn.*, vol. 59, no. 2, Feb. 2023, Art. no. 8200205.

[22] G. W. Jewell and D. Howe, "Computer-aided design of magnetizing fixtures for the post-assembly magnetization of rare-earth permanent magnet brushless DC motors," *IEEE Trans. Magn.*, vol. 28, no. 5, pp. 3036–3038, Sep. 1992.

[23] M.-F. Hsieh, Y.-C. Hsu, and D. G. Dorrell, "Design of large-power surface-mounted permanent-magnet motors using postassembly magnetization," *IEEE Trans. Ind. Electron.*, vol. 57, no. 10, pp. 3376–3384, Oct. 2010.

[24] M.-F. Hsieh, Y.-C. Hsu, and P.-T. Chen, "Analysis and experimental study of permanent magnet machines with in-situ magnetization," *IEEE Trans. Magn.*, vol. 49, no. 5, pp. 2351–2354, May 2013.

[25] M.-F. Hsieh, D. G. Dorrell, C.-K. Lin, P.-T. Chen, and P. Y. P. Wung, "Modeling and effects of in situ magnetization of isotropic ferrite magnet motors," *IEEE Trans. Ind. Appl.*, vol. 50, no. 1, pp. 364–374, Jan. 2014.

[26] M.-F. Hsieh, Y.-M. Lien, and D. G. Dorrell, "Post-assembly magnetization of rare-earth fractional-slot surface permanent-magnet machines using a two-shot method," *IEEE Trans. Ind. Appl.*, vol. 47, no. 6, pp. 2478–2486, Nov. 2011.

[27] M.-J. Jeong, K.-B. Lee, H.-J. Pyo, D.-W. Nam, and W.-H. Kim, "A study on the shape of the rotor to improve the performance of the spoke-type permanent magnet synchronous motor," *Energies*, vol. 14, no. 13, p. 3758, Jun. 2021.

[28] M.-J. Jeong, H.-J. Pyo, D.-W. Nam, and W.-H. Kim, "A study on a ferrite spoke-type permanent magnet synchronous motor with improved post-assembly magnetization performance," in *Proc. IEEE 20th Biennial Conf. Electromagn. Field Comput. (CEFC)*, Denver, CO, USA, Oct. 2022, pp. 1–2.

[29] K.-S. Kim, M.-R. Park, H.-J. Kim, S.-H. Chai, and J.-P. Hong, "Estimation of rotor type using ferrite magnet considering the magnetization process," *IEEE Trans. Magn.*, vol. 52, no. 3, Mar. 2016, Art. no. 8101804.

[30] Y. Kawase, T. Yamaguchi, N. Mimura, M. Igata, and K. Ida, "Analysis of magnetizing process using discharge current of capacitor by 3-D finite-element method," *IEEE Trans. Magn.*, vol. 38, no. 2, pp. 1145–1148, Mar. 2002.

[31] F. Liu, D. Li, Y. Wang, Y. Li, Z. Zhao, and Q. Yang, "Analysis of Magnetizing Process Using the Discharge Current of Capactor by $T-\Omega$ Method," *IEEE Trans. Magn.*, vol. 26, no. 4, Jun. 2016, Art. no. 0603504.

[32] H.-S. Seol, T.-C. Jeong, H.-W. Jun, J. Lee, and D.-W. Kang, "Design of 3-times magnetizer and rotor of spoke-type PMSM considering post-assembly magnetization," *IEEE Trans. Magn.*, vol. 53, no. 11, Nov. 2017, Art. no. 8208005.

[33] J.-W. Jung, "Rotor," US 9 800 107 B2, Oct. 24, 2017.

[34] K. Yamazaki and N. Fukushima, "Torque and loss calculation of rotating machine considering laminated cores using post 1-D analysis," *IEEE Trans. Magn.*, vol. 47, no. 5, pp. 994–997, May 2011.

SEONG-JIN KWON received the B.S. and M.S. degrees in mechanical engineering and the Ph.D. degree in mechanical design from Sungkyunkwan University, Suwon, South Korea, in 2000, 2002, and 2005, respectively.

He was a Visiting Researcher with The University of Tokyo, Japan, from 2002 to 2003, and The University of New South Wales, Australia, in 2004. From 2006 to 2023, he was an Executive Principal Researcher and the Director of the Vehicle Safety Research and Development Center, Korea Automotive Technology Institute (KATECH). Since 2023, he has been with Yeungnam University, Gyeongsan, South Korea, where he is currently an Assistant Professor. His research interests include vehicle dynamics and control and next-generation vehicle design.

BYEONG-HWA LEE (Member, IEEE) received the B.S. degree in electrical engineering from Changwon National University, Changwon, South Korea, in 2006, and the M.S. and Ph.D. degrees in automotive engineering from Hanyang University, Seoul, South Korea, in 2009 and 2013, respectively.

Since 2013, she has been a Senior Engineer with the Electric Power Train Center, Korea Automotive Research Institute (KATECH), Daegu, South Korea. Her research interest includes the design and analysis of traction motors for electric vehicles.

KYU-SEOB KIM received the bachelor's degree in mechanical engineering and the master's and Ph.D. degrees in automotive engineering from Hanyang University, Seoul, South Korea, in 2010, 2012, and 2016, respectively. From 2016 to 2022, he was the Principle Researcher with the Tuning Parts Research and Development Center, Korea Automotive Technology Institute, Daegu, South Korea. Since 2022, he has been with Gyeongsang National University, Jinju, South Korea, where he is currently an Assistant Professor. His research interests include electromagnetic field analysis and electric machinery of automotive systems.

JAE-WOO JUNG (Member, IEEE) received the B.S. and M.S. degrees in electrical engineering from Changwon National University, Changwon, South Korea, in 2005 and 2007, respectively, and the Ph.D. degree in automotive engineering from Hanyang University, Seoul, South Korea, in 2013. From 2009 to 2012, he developed PMSM for automotive applications with S&T Motiv Company Ltd. Since 2013, he has been a Research Staff Member with the Research and Development Center, Hyundai Mobis Company Ltd., Yongin, South Korea. Since 2021, he has been an Assistant Professor with Daegu University, Gyeongsan, South Korea. His research interests include the design and analysis of various electromagnetic devices for electromechanical components of automotive applications and the design of electric motors for electric powertrain systems.